Does a Quark-Gluon Plasma Feature an Extended Hydrodynamic Regime?

Weiyao Ke[1,*] and Yi Yin[2,†]
[1]Theoretical Division, Los Alamos National Laboratory, Los Alamos, New Mexico 87545, USA
[2]Quark Matter Research Center, Institute of Modern Physics, Chinese Academy of Sciences, Lanzhou 730000, China

(Received 24 August 2022; revised 21 February 2023; accepted 27 April 2023; published 26 May 2023)

We investigate the response of the near-equilibrium quark-gluon plasma (QGP) to perturbation at nonhydrodynamic gradients. We propose a conceivable scenario under which sound mode continues to dominate the medium response in this regime. Such a scenario has been observed experimentally for various liquids and liquid metals. We further show that this extended hydrodynamic regime (EHR) indeed exists for both the weakly coupled kinetic equation in the relaxation time approximation (RTA) and the strongly coupled $\mathcal{N} = 4$ supersymmetric Yang-Mills (SYM) theory. We construct a simple but nontrivial extension of Müller-Israel-Stewart (MIS) theory—namely MIS*—and demonstrate that it describes the EHR response for both the RTA and SYM theory. This indicates that MIS* equations can potentially be employed to search for QGP EHR via heavy-ion collisions.

DOI: 10.1103/PhysRevLett.130.212303

Introduction.—The properties of many-body QCD systems, particularly their behavior at different scales, have fascinated high-energy nuclear physicists for decades. One prominent example of such a system is quark-gluon plasma (QGP) that is created in a heavy-ion collision (HIC) [1]. The remarkable and nontrivial agreement between hydrodynamic modeling and many results of HIC [2,3] indicates that the asymptotically free QGP behaves as a near-perfect fluid at long distances. However, much less is known about its properties at the intermediate scale, where the characteristic length is too short for a fluid description and is too long to be treated perturbatively [4].

One central question, which we shall concentrate on, is how an equilibrated QGP responds to an external disturbance with varying gradients. When the perturbation varies slowly in space and time, the hydrodynamic modes, such as sound and shear modes, dominate the response after a sufficiently long time. In this hydrodynamic regime (HR), the medium's behavior is described by viscous hydrodynamics. The description beyond the HR, in general, can be exceedingly complex. It is commonly assumed that dynamics in such situations involve a tower of nonhydrodynamic excitations [5].

Nevertheless, an alternative scenario may and does exist in condensed matter systems. Since the seminal measurement in Ref. [6], there is mounting empirical evidence showing that a variety of liquids and liquid metals, such as liquid zinc [7] and liquid K-Cs alloys [8], can sustain sound modes extending from the HR to wavelengths comparable to interatomic separations; see Refs. [9,10] for reviews. Though the physical origins of those so-called "high wave vector" sound modes are still under intensive investigation, they are found to be essential for understanding the properties of the material at nonhydrodynamic wavelengths (see, e.g., Ref. [8]).

The above observations exemplify the situation in which the damping rate of hydrodynamic excitations remains smaller than other excitations up to some critical wave number q_c beyond HR. In such an extended hydrodynamic regime (EHR), hydrodynamic modes still dominate the response at a timescale longer than the inverse of the gap (in damping rate), despite the fact that viscous hydrodynamics is not expected to describe their dispersion (see also Ref. [11]). As we shall see explicitly below, an EHR exists in representative microscopic theories such as the kinetic theory under the relaxation time approximation (RTA) and the strongly coupled $\mathcal{N} = 4$ supersymmetric Yang-Mills theory in the large-N_c limit (SYM), indicating the generality of the EHR regardless of the coupling strength.

In this Letter, we propose an EHR as a conceivable scenario for QGP; i.e., sound modes may dominate the near-equilibrium response at a significant gradient. What would we learn about QGP if such an EHR existed? First, if we suppose so, the characterization of QGP at intermediate scales is simplified, since we can describe medium properties in the EHR with a few parameters such as effective sound velocity and attenuation rate. Second, it will fill the gap in our knowledge about the emergence of QGP liquid from asymptotic parton gas.

Can we test the EHR scenario of QGP experimentally? In HIC, the azimuthal asymmetries in the flow of produced hadrons v_n have been measured and are commonly interpreted as the response to the initial eccentricity. In smaller colliding systems, eccentricities are dominated by shorter-scale fluctuations, and the EHR response can be responsible for v_n generation. In fact, describing observed collectivity in those small colliding systems from nonhydrodynamic transport has already attracted considerable attention [5,12]. Besides this, the medium response to jet

propagation can be another channel to probe the EHR behavior. In Refs. [13–15], it was found that energy and momentum deposited by fast partons cause large gradient perturbations, and the excited medium response is correlated nontrivially with jet production.

A phenomenological investigation of the QGP EHR requires extending the standard hydrodynamic modeling of HIC to incorporate the EHR response. To date, no serious attempt to construct such a model has been made. We shall propose a simple but nontrivial extension of Müller-Israel-Stewart (MIS) theory, which we call MIS*, for this purpose. As we shall demonstrate, MIS* can successfully describe the EHR response for different microscopic theories for the static and Bjorken expanding background. We believe our construction to be an essential first step toward the experimental search for an EHR.

EHR in weakly and strongly coupled theories.—We now demonstrate the presence of an EHR for two representative microscopic theories—namely, RTA kinetic theory and SYM.

In the RTA kinetic theory, the distribution function $f(t,\boldsymbol{x},\boldsymbol{p})$ obeys

$$p^\mu \partial_\mu f - \Gamma^\lambda_{\alpha\sigma} p^\alpha p^\sigma \frac{\partial f}{\partial p^\lambda} = -\frac{u\cdot p}{\tau_R}(f - f_{\rm eq}). \tag{1}$$

Here, $\Gamma^\lambda_{\alpha\beta}$ denotes the metric connection. The relaxation time τ_R controls the timescale at which f approaches the equilibrium distribution $f_{\rm eq} = e^{\beta p\cdot u}$, where β and u^μ denote inverse temperature and fluid velocity, respectively. For a conformal liquid, $\tau_R \propto \epsilon^{-1/4}$, with ϵ being the local energy density. The dispersion of the sound mode can be obtained from solving [16]

$$(\mathfrak{q}^2 + iC_\pi \mathfrak{w}) + \frac{iC_\pi}{2\mathfrak{q}}[\mathfrak{q}^2 + 3\mathfrak{w}(iC_\pi + \mathfrak{w})L] = 0. \tag{2}$$

Here, we use the dimensionless frequency $\mathfrak{w} \equiv \omega\nu$ and wave vector $\mathfrak{q} = \nu q$, where $\nu = 4\eta_0/3(\epsilon_0 + p_0)$, with η_0 being the shear viscosity, ϵ_0 the energy density, and p_0 the pressure of the background. $L = \ln(\mathfrak{w} - \mathfrak{q} + iC_\pi/\mathfrak{w} + \mathfrak{q} + iC_\pi)$, and the dimensionless ratio $C_\pi \equiv \tau_\pi/\nu$ is related to the shear relaxation time τ_π. For RTA kinetic theory, $\nu = 4\tau_R/15$ and $C_\pi = 15/4$ [16], while for SYM, $\nu = \beta/3\pi$, $C_\pi = 3(2-\log 2)/2$ [17].

Turning to SYM, we employ the AdS/CFT correspondence, which maps the correlator in the quantum field theory in d-dimensional space-time into a classical general relativity calculation in $d+1$ dimensions. The excitations in the sound channel can be found by solving [18,19]

$$Z'' - \frac{3\mathfrak{w}^2(1+\mathfrak{u}^2) + \mathfrak{q}^2(2\mathfrak{u}^2 - 3\mathfrak{u}^4 - 3)}{\mathfrak{u}(1-\mathfrak{u}^2)(3\mathfrak{w}^2 + \mathfrak{q}^2(\mathfrak{u}^2-3))} Z' + \frac{4}{9}\times \frac{3\mathfrak{w}^4 + \mathfrak{q}^4(3 - 4\mathfrak{u}^2 + \mathfrak{u}^4) + \mathfrak{q}^2(9\mathfrak{u}^5 - 9\mathfrak{u}^3 + 4\mathfrak{u}^2\mathfrak{w}^2 - 6\mathfrak{w}^2)}{\mathfrak{u}(1-\mathfrak{u}^2)^2(3\mathfrak{w}^2 + \mathfrak{q}^2(\mathfrak{u}^2-3))} Z = 0, \tag{3}$$

where $Z(\mathfrak{u})$ depends on the radial coordinate $\mathfrak{u}$ of the extra dimension. Equation (3) has to be solved with the infalling wave boundary condition $Z \sim (1-\mathfrak{u})^{-i\mathfrak{w}/3}$, as $\mathfrak{u} \to 1$ (horizon). Near the boundary $\mathfrak{u} = 0$, $Z(\mathfrak{u}) \sim \mathcal{A}(\mathfrak{q},\mathfrak{w})(1+\cdots) + \mathcal{B}(\mathfrak{q},\mathfrak{w})\mathfrak{u}^2 + \cdots$, where the dots denote higher powers of $\mathfrak{u}$. The Dirichlet boundary condition $\mathcal{A}(\mathfrak{q},\mathfrak{w}) = 0$ determines the dispersion relation of excitations, which we obtained from the public *Mathematica* code given by Ref. [20].

In Fig. 1, we present the sound dispersion relation $\mathfrak{w}_\pm(\mathfrak{q}) = \pm v(\mathfrak{q})\mathfrak{q} - i\Gamma(\mathfrak{q})$ in RTA kinetic theory (left) and SYM (right). The phase velocity v and sound attenuation rate Γ are shown in red solid curves in the upper and lower panels, respectively. Also shown are representative nonhydrodyamic excitations in the black dashed curve. For comparison, we consider the dispersion of excitations in the sound channel in MIS theory [21,22]:

$$\mathfrak{w}^2 - c_s^2\mathfrak{q}^2 + \frac{i\mathfrak{w}\mathfrak{q}^2}{(1 - iC_\pi\mathfrak{w})} = 0, \tag{4}$$

where sound velocity $c_s^2 = 1/3$ for the two theories studied in this section. In the limit $C_\pi \to 0$, Eq. (4) reduces to the familiar expression in first-order hydrodynamic $\mathfrak{w}^2 - c_s^2\mathfrak{q}^2 + i\mathfrak{w}\mathfrak{q}^2 = 0$. Sound dispersion in first-order hydrodynamics and MIS, obtained by solving Eq. (4) with $C_\pi = 0$ and fixed C_π, are shown in blue dotted and green dashed curves, respectively, in Fig. 1. Plotting them at a nonhydrodynamic gradient will tell us the regime where conventional hydrodynamic theories cease to be a good description of the response.

For RTA kinetic theory, the sound modes are gapped from the quasiparticle excitations with damping rate τ_R^{-1}, up to a critical value $\mathfrak{q}_c = 1.2$ [16]. Far below $\mathfrak{q}_c$, the sizable difference from first-order hydrodynamics is seen in the damping rate, and even more so in the phase velocity, even for $\mathfrak{q} > 0.2$. Therefore, $0.2 < \mathfrak{q} < 1.2$ may be viewed as an EHR for RTA kinetic theory.

As for SYM, the gap between sound modes and nonhydrodynamic excitations, a tower of quasinormal modes, remains open for any $\mathfrak{q}$ under study (see also Refs. [19,23]). The first-order hydrodynamics fails to describe the dispersion, notably for the phase velocity at $\mathfrak{q} > 0.3$. So, we conclude that the EHR also exists in SYM and corresponds to $\mathfrak{q} > 0.3$. Besides this, an EHR can be identified in other strongly coupled theories—e.g., Ref. [24]. For the effectiveness of the hydrodynamic description of the nonequilibrium bulk evolution in the same SYM theory, see Refs. [25–29]. Note that previous works on SYM dispersion [30–32] consider the collision of complex hydrodynamic modes with

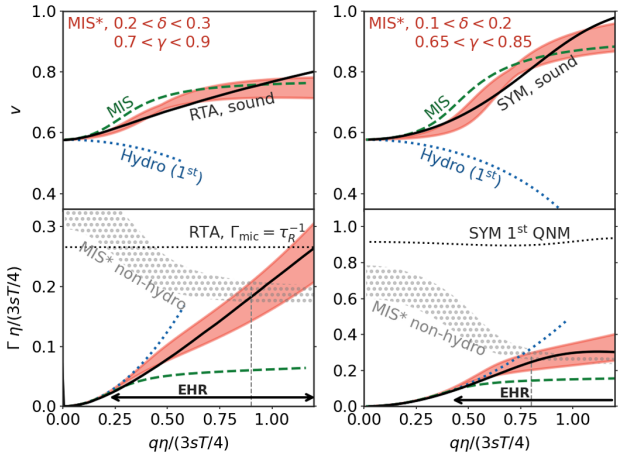

FIG. 1. Sound phase velocity (the upper panel) and damping rate Γ (the lower panel) as a function of gradient $\mathfrak{q}$ for RTA kinetic theory (left) and strongly coupled SYM (right). The damping rate of representative nonhydrodynamic excitations is shown in black dotted curves. The gap between those excitations and sound modes at a nonhydrodynamic gradient indicates the existence of an extended hydrodynamic regime (EHR). The first-order hydrodynamic and MIS results, shown in blue dotted and green dashed curves, respectively, fail to capture the key features of sound modes in an EHR. In contrast, for a given range of model parameters (red bands), MIS* efficiently describes EHR sound propagation up to some value q_c (the dashed horizontal lines in the lower panel).

nonhydrodynamic ones at some complex q, while the present Letter analyzes the gap in the decay rate (the imaginary part of the frequency) at real q.

We summarize features that kinetic and SYM theory share in the EHR. First, the phase velocity, or the "effective stiffness," becomes supersonic, $v \geq \sqrt{1/3}$. Second, the damping rate $\Gamma(q)$ is always smaller than that of the first-order hydrodynamics at fixed $\mathfrak{q}$. These behaviors may be anticipated on physical grounds as follows: As gradient $\mathfrak{q}$ grows, more and more d.o.f.'s fall out of equilibrium and cannot respond to the compression, resulting in larger stiffness—i.e., a larger effective sound velocity. At the same time, those off-equilibrium d.o.f.'s would not contribute to the dissipative process, leading to a smaller damping rate relative to that of the first-order hydrodynamics. The above picture is admittedly speculative, but it illustrates that studying sound propagation can be instrumental in characterizing medium properties in an EHR.

Dynamical models for an EHR.—Building dynamical models with an EHR response is necessary for searching for an EHR through data-modeling comparison. The commonly used MIS theory or other variants of second-order hydrodynamics are not suitable for the present purpose. As shown in Fig. 1, MIS results only show a modest improvement compared with first-order hydrodynamics but generically underestimate the attenuation in the EHR. Adding higher-order gradient terms [30–34] (see also Refs. [35–37] for other attempts to improve hydrodynamics) is systematic in principle, though it would proliferate input parameters.

Instead, we aim at constructing a model such that (*a*) it reduces to viscous hydrodynamics in the long-wavelength limit, and (*b*) for a given microscopic theory, it could describe sound propagation in EHR (or part of it) with a minimum number of model parameters. Below, we propose an extension of the MIS equation, MIS*, containing two key additional model parameters as compared with first-order hydrodynamics and demonstrate that it serves the purpose. Our construction is partly inspired by the Hydro + framework [38].

MIS.*—Consider the decomposition of the stress-energy tensor $T^{\mu\nu} = T^{\mu\nu}_{(0)} + \pi^{\mu\nu}$, where $T^{\mu\nu}_{(0)} = \epsilon u^\mu u^\nu + p\Delta^{\mu\nu}$ denotes the ideal fluid part with $\Delta^{\mu\nu} = g^{\mu\nu} + u^\mu u^\mu$. In viscous hydrodynamics, the nonequilibrium corrections to $T^{\mu\nu}$, $\pi^{\mu\nu}$, become $\pi^{\mu\nu}_{(1)} = \eta\sigma^{\mu\nu}$, where $\sigma^{\mu\nu} = \partial^\mu_\perp u^\nu + \partial^\mu_\perp u^\nu - (2/3)\Delta^{\mu\nu}\theta$, with $\theta = \partial \cdot u, \partial^\mu_\perp \equiv \Delta^{\mu\nu}\partial_\nu$. For simplicity, we shall consider a uncharged and conformal fluid so that $\pi^{\mu\nu}$ is traceless. The MIS theory treats $\pi^{\mu\nu}$ as a dynamical variable which relaxes to $\pi^{\mu\nu}_{(1)}$ at timescale τ_π. However, in an EHR where the timescale can be shorter than τ_π, $\pi^{\mu\nu}$ falls out of equilibrium and does not contribute to the dissipation. As a result, the EHR sound is underdamped in MIS.

To describe sound propagation better, in MIS*, we divide $\pi^{\mu\nu}$ into two parts:

$$\pi^{\mu\nu} = \pi^{\mu\nu}_s + \pi^{\mu\nu}_f, \tag{5}$$

and we evolve π_s, π_f at different relaxation times τ'_π, τ''_π. By design, we require $\tau'_\pi \gg \tau''_\pi$ such that in an EHR regime, the typical timescale is comparable to or shorter than τ'_π but is much longer than τ''_π. Consequently, in the EHR, $\pi^{\mu\nu}_f$ should approach a fixed form, which we take to be $\eta'\sigma^{\mu\nu}$. Here, $\eta' < \eta$ controls the effective viscosity in the EHR. Explicitly, we propose the following equations:

$$(u\cdot\partial)\pi^{\mu\nu}_s = -\frac{\pi^{\mu\nu}_s + (\eta-\eta')\sigma^{\mu\nu}}{\tau'_\pi} + R, \tag{6}$$

$$(u\cdot\partial)\pi^{\mu\nu}_f = -\frac{\pi^{\mu\nu}_f + \eta'\sigma^{\mu\nu}}{\tau''_\pi}, \tag{7}$$

where $R = -\frac{4}{3}\pi^{\mu\nu}_s\theta + \cdots$ denotes other possible second-order gradient terms which do not contribute to the sound dispersion. We may practically fix R by requiring Eq. (6) to become BRSSS second-order hydrodynamics [17] or its variants in the limit $\eta' = 0$.

Equations (6) and (7) together with $\partial_\mu T^{\mu\nu} = 0$ constitute MIS* equations. In a timescale longer than τ'_π, $\pi^{\mu\nu}_s \to (\eta-\eta')\sigma^{\mu\nu}$, $\pi^{\mu\nu}_f \to \eta'\sigma^{\mu\nu}$, $R \to 0$, and hence MIS* reduces to the first-order fluid dynamics. If we take the limit $\tau''_\pi \to 0$, $\pi^{\mu\nu}_f$ becomes $\eta'\sigma^{\mu\nu}$ and is no longer dynamical. This is the limit we shall use below for illustration, though

in a realistic simulation of MIS*, a finite τ_π'' is needed to ensure causality.

*Sound mode in MIS**.—The excitations in the sound channel are given by

$$\mathfrak{w}^2 - c_s^2\mathfrak{q}^2 + i\left[\delta + \frac{(1-\delta)}{(1-i\gamma C_\pi \mathfrak{w})}\right]\mathfrak{w}\mathfrak{q}^2 = 0, \tag{8}$$

where $(\delta,\gamma) = (\eta'/\eta, \tau_\pi'/\tau_\pi)$. Note that for $(\delta,\gamma) = (0,1)$, Eq. (8) reduces to Eq. (4). Similarly to MIS theory, the excitations of MIS* in the sound channel include a pair of sound modes and a dissipative mode. The boundary of the EHR is determined by the "level-crossing point" q_c', where the sound damping rate equals that of the dissipative mode. In Fig. 1 in the Supplemental Material [39], we show the dependence of dispersion on δ, γ and find that by tuning them, MIS* has the flexibility and capability of describing a class of sound propagation up to q_c'.

The comparison between sound dispersion in MIS* and that in RTA and SYM theory, as shown in Fig. 1, is encouraging. For $0.2 < \delta < 0.3$, $0.7 < \gamma < 0.9$, MIS* describes the RTA sound mode well up to $\mathfrak{q} \sim \mathfrak{q}_c' = 0.95$. For a SYM system, a different range—$0.1 < \delta < 0.2$, $0.65 < \gamma < 0.85$—provides a reasonable description up to $\mathfrak{q}_c' = 0.7$. Given its simplicity, we do not anticipate the MIS* covering the full EHR in the two microscopic theories. Notwithstanding, MIS* extends the description from the HR to a significant part of the EHR in both cases.

Bjorken expansion.—One advantage of MIS* is that once its model parameters are fixed by matching to sound dispersion, it can readily be applied to an expanding background. Now, we consider a linearized response for a boost-invariant Bjorken expanding background specified by the evolution of $\epsilon_0(\tau)$ vs Bjorken time τ. For simplicity, we assume that perturbations only depend on $\boldsymbol{y}$, the spatial vector lying in the plane transverse to the z direction (longitudinal direction). The response of $T^{\mu\nu}$ is characterized by several independent response functions [40]. Below, we focus on the energy-energy response function $\mathcal{G}_{\epsilon\epsilon}$ which evolves the initial energy perturbation $\delta\epsilon(\tau',\boldsymbol{y}')$ to

$$\delta\epsilon(\tau,\boldsymbol{y}) = \int d^2\boldsymbol{y}'\mathcal{G}_{\epsilon\epsilon}(r;\tau,\tau')\delta\epsilon(\tau',\boldsymbol{y}'), \tag{9}$$

where $\boldsymbol{r} \equiv \boldsymbol{y} - \boldsymbol{y}'$. To obtain $\mathcal{G}_{\epsilon\epsilon}$ in RTA theory, we expand the distribution function $f(\tau,\boldsymbol{y};\boldsymbol{p}) = f_0(\tau;\boldsymbol{p}) + \delta f(\tau,\boldsymbol{y};\boldsymbol{p})$. Since the plasma starts equilibrating for $\tau > \tau_R$ (cf. Fig. 1 in Ref. [41]), we first determine the background solution $f_0(\tau;\boldsymbol{p})$ with a relaxation time $\tau_R(\tau) \propto \epsilon(\tau)^{-1/4}$ starting from $\tau_0 = \tau_R(\tau_0)$ [corresponding to $\tau_0 T/(4\pi\eta/s) = 0.40$]. Then, the linearized RTA equation [Eq. (1)] is solved numerically to obtain $\mathcal{G}_{\epsilon\epsilon}(q;\tau,\tau')$ in Fourier space. Because of the large-q spurious wave behavior in MIS theory, a smearing function $\exp\{-q^2/[2(4/\tau_0)^2]\}$ is applied when transforming q-space results back to the $\boldsymbol{y}$ space.

In Fig. 2, we take $\tau' = 2\tau_0$, meaning we are considering the near-equilibrium rather than the far-from-equilibrium expanding plasma [41], and we show $\mathcal{G}_{\epsilon\epsilon}$ at three representative times $\Delta\tau = 2, 8, 16\tau_0$ as a function of $r/\Delta\tau$ where $\Delta\tau = \tau - \tau'$. The RTA response functions are then compared to first-order, MIS, and MIS* theory; see our forthcoming paper for further details. The hydrodynamic curves approach the kinetic ones at a very late time, say $\tau = 16\tau_0$, but their differences are significant earlier. Particularly, the peak of $\mathcal{G}_{\epsilon\epsilon}$,$(r/\Delta\tau)_{\text{peak}}$ approaches $c_s = \sqrt{1/3}$ as τ grows, but it is always larger than c_s, in accordance with the supersonic nature of EHR sound propagation. Rather than improving the description at early times, the MIS theory introduces spurious shocks; see also Ref. [42]. This can be understood from Fig. 1, where we see that MIS underestimates the sound attenuation in the EHR. Remarkably, with the same range of δ, γ as used to reproduce the EHR

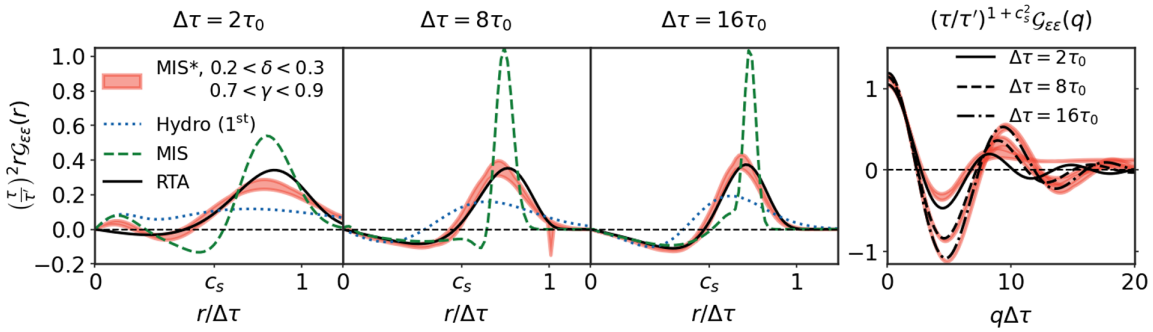

FIG. 2. The left three panels show the real-space energy-energy response function $\mathcal{G}_{\epsilon\epsilon}(r)$ [defined in Eq. (9) and multiplied by $(\tau/\tau')^2 r$)] plotted as a function of $r/\Delta\tau$ for the Bjorken expanding plasma. RTA kinetic theory, first-order hydrodynamics, and MIS theory results are shown by the solid, dotted, and dashed curves, respectively. The MIS* results, computed from the same range of model parameters δ, γ as used in the left panels of Fig. 1 (left), are plotted in the red band. Three values of $\Delta\tau$ are chosen to represent the response function at early, intermediate, and late time (from left to right). In the hydrodynamic limit, the peak location of $\mathcal{G}_{\epsilon\epsilon}(r)$ should approach $c_s = 1/\sqrt{3}$. In the fourth panel, we compare the q-space energy-energy response function of the RTA theory and MIS*.

sound dispersion, MIS* response functions generally agree with RTA results from early to late times. For a reference, the comparison between MIS* and RTA in the q space is shown in the rightmost panel of Fig. 2. Equally impressive agreement is seen for several other energy-momentum response functions; see Fig. 3 in the Supplemental Material [39]. This convincingly indicates that describing EHR sound propagation is key to characterizing system response beyond the conventional hydrodynamic regime, and MIS* serves that purpose.

Summary.—We consider the extended hydrodynamic regime (EHR) scenario for QGP, where sound modes are gapped from other excitations at a nonhydrodynamic gradient. We construct hydrodynamic-like equations, MIS*, and demonstrate that they describe sound propagation in RTA and SYM theories in the EHR. This indicates that MIS*, with suitable refinement, can be employed in future quantitative studies of small colliding systems [43] and jet-medium response [13–15] and in the empirical search of the EHR. In parallel, the EHR scenario can be directly tested for weakly coupled QGP by examining the sound mode in the QCD effective kinetic theory [44].

The current study concentrates on the sound channel. In the Supplemental Material [39], we briefly demonstrate that the notion of the EHR can be equally applied to the shear channel for both RTA kinetic theory and SYM. In the future, one may consider the effects of hydrodynamic noise and the situations where there are additional nonhydrodynamic slow modes in HR.

Compared to the intensive studies of far-from-equilibrium hydrodynamics and the associated attractor behavior in the early-stage bulk evolution of heavy-ion collisions [45,46], the present work focuses on the linearized response of large-gradient perturbations in a near-equilibrium medium. In the view that a large $1/\tau$ at early times implies a large gradient, a connection between the bulk-evolution attractor and the EHR is worthy of exploring. For example, one may investigate if MIS* can describe far-from-equilibrium response function [40,41]. We leave those for the future.

We thank Xiaojian Du, Shu Lin, Krishna Rajagopal, and Li Yan for valuable discussions, and Matteo Baggioli, Michal Heller, Lipei Du, Ulrich Heinz, and Soeren Schlichting for helpful comments on the draft. W. K. is supported by the U.S. Department of Energy through the Office of Nuclear Physics and the LDRD program at Los Alamos National Laboratory (W. K.). Los Alamos National Laboratory is operated by Triad National Security, LLC, for the National Nuclear Security Administration of the U.S. Department of Energy (Contract No. 89233218CNA000001). Y. Y. acknowledges the support from the Strategic Priority Research Program of the Chinese Academy of Sciences, Grant No. XDB34000000 and NSFC under Grant No. 12175282.

*weiyaoke@lanl.gov
†yiyin@impcas.ac.cn

[1] K. Adcox *et al.* (PHENIX Collaboration), Nucl. Phys. **A757**, 184 (2005).
[2] U. W. Heinz, J. Phys. Conf. Ser. **455**, 012044 (2013).
[3] B. Schenke, Rep. Prog. Phys. **84**, 082301 (2021).
[4] W. Busza, K. Rajagopal, and W. van der Schee, Annu. Rev. Nucl. Part. Sci. **68**, 339 (2018).
[5] A. Kurkela, U. A. Wiedemann, and B. Wu, Eur. Phys. J. C **79**, 965 (2019).
[6] J. R. D. Copley and J. M. Rowe, Phys. Rev. Lett. **32**, 49 (1974).
[7] M. Zanatta, F. Sacchetti, E. Guarini, A. Orecchini, A. Paciaroni, L. Sani, and C. Petrillo, Phys. Rev. Lett. **114**, 187801 (2015).
[8] L. E. Bove, F. Sacchetti, C. Petrillo, and B. Dorner, Phys. Rev. Lett. **85**, 5352 (2000).
[9] T. Scopigno, G. Ruocco, and F. Sette, Rev. Mod. Phys. **77**, 881 (2005).
[10] K. Trachenko and V. V. Brazhkin, Rep. Prog. Phys. **79**, 016502 (2015).
[11] M. Baggioli, M. Vasin, V. V. Brazhkin, and K. Trachenko, Phys. Rep. **865**, 1 (2020).
[12] A. Kurkela, A. Mazeliauskas, and R. Törnkvist, J. High Energy Phys. 11 (2021) 216.
[13] Y. Tachibana, N.-B. Chang, and G.-Y. Qin, Phys. Rev. C **95**, 044909 (2017).
[14] W. Chen, S. Cao, T. Luo, L.-G. Pang, and X.-N. Wang, Phys. Lett. B **777**, 86 (2018).
[15] S. Cao and X.-N. Wang, Rep. Prog. Phys. **84**, 024301 (2021).
[16] P. Romatschke, Eur. Phys. J. C **76**, 352 (2016).
[17] R. Baier, P. Romatschke, D. T. Son, A. O. Starinets, and M. A. Stephanov, J. High Energy Phys. 04 (2008) 100.
[18] P. K. Kovtun and A. O. Starinets, Phys. Rev. D **72**, 086009 (2005).
[19] I. Amado, C. Hoyos-Badajoz, K. Landsteiner, and S. Montero, J. High Energy Phys. 07 (2008) 133.
[20] A. Jansen, Eur. Phys. J. Plus **132**, 546 (2017).
[21] P. Romatschke, Int. J. Mod. Phys. E **19**, 1 (2010).
[22] J. Hong and D. Teaney, Phys. Rev. C **82**, 044908 (2010).
[23] J. F. Fuini, C. F. Uhlemann, and L. G. Yaffe, J. High Energy Phys. 12 (2016) 042.
[24] M. Edalati, J. I. Jottar, and R. G. Leigh, J. High Energy Phys. 10 (2010) 058.
[25] P. M. Chesler and L. G. Yaffe, Phys. Rev. D **82**, 026006 (2010).
[26] M. P. Heller, R. A. Janik, and P. Witaszczyk, Phys. Rev. Lett. **108**, 201602 (2012).
[27] P. M. Chesler, Phys. Rev. Lett. **115**, 241602 (2015).
[28] J. Casalderrey-Solana, M. P. Heller, D. Mateos, and W. van der Schee, Phys. Rev. Lett. **111**, 181601 (2013).
[29] J. Casalderrey-Solana, M. P. Heller, D. Mateos, and W. van der Schee, Phys. Rev. Lett. **112**, 221602 (2014).
[30] B. Withers, J. High Energy Phys. 06 (2018) 059.
[31] S. Grozdanov, P. K. Kovtun, A. O. Starinets, and P. Tadić, Phys. Rev. Lett. **122**, 251601 (2019).
[32] S. Grozdanov, P. K. Kovtun, A. O. Starinets, and P. Tadić, J. High Energy Phys. 11 (**2019**) 097.

[33] M. P. Heller, A. Serantes, M. Spaliński, V. Svensson, and B. Withers, Phys. Rev. D **104**, 066002 (2021).
[34] M. P. Heller, A. Serantes, M. Spaliński, V. Svensson, and B. Withers, SciPost Phys. **10**, 123 (2021).
[35] M. Lublinsky and E. Shuryak, Phys. Rev. D **80**, 065026 (2009).
[36] M. P. Heller, R. A. Janik, M. Spaliński, and P. Witaszczyk, Phys. Rev. Lett. **113**, 261601 (2014).
[37] M. P. Heller, A. Serantes, M. Spaliński, V. Svensson, and B. Withers, Phys. Rev. X **12**, 041010 (2022).
[38] M. Stephanov and Y. Yin, Phys. Rev. D **98**, 036006 (2018).
[39] See Supplemental Material at http://link.aps.org/supplemental/10.1103/PhysRevLett.130.212303 for we present some calculation details, including the dependence of dispersion relation on MIS* parameters, the extended hydrodynamic regime in the shear channel and other energy-momentum response functions.
[40] A. Kurkela, A. Mazeliauskas, J.-F. Paquet, S. Schlichting, and D. Teaney, Phys. Rev. C **99**, 034910 (2019).
[41] S. Kamata, M. Martinez, P. Plaschke, S. Ochsenfeld, and S. Schlichting, Phys. Rev. D **102**, 056003 (2020).
[42] J. Hong, D. Teaney, and P. M. Chesler, Phys. Rev. C **85**, 064903 (2012).
[43] J. L. Nagle and W. A. Zajc, Annu. Rev. Nucl. Part. Sci. **68**, 211 (2018).
[44] L. Keegan, A. Kurkela, A. Mazeliauskas, and D. Teaney, J. High Energy Phys. 08 (**2016**) 171.
[45] M. P. Heller and M. Spalinski, Phys. Rev. Lett. **115**, 072501 (2015).
[46] P. Romatschke, Phys. Rev. Lett. **120**, 012301 (2018).